Available online at www.sciencedirect.com
SCIENCE DIRECT®
Experimental Cell Research 297 (2004) 363–379
Experimental Cell Research
www.elsevier.com/locate/yexcr

Improvement of calcium handling and changes in calcium-release properties after mini- or full-length dystrophin forced expression in cultured skeletal myotubes

Eric Marchand,[a] Bruno Constantin,[a,*] Haouaria Balghi,[a] Marie-Christine Claudepierre,[b] Anne Cantereau,[a] Christophe Magaud,[a] Aklesso Mouzou,[a] Guy Raymond,[a] Serge Braun,[b] and Christian Cognard[a]

[a] *Institut de Physiologie et Biologie Cellulaire, UMR CNRS/Université de Poitiers 6187, Pôle Biologie Santé, 86022 Poitiers cedex, France*
[b] *Transgene S. A., 67082 Strasbourg cedex, France*

Received 30 May 2003, revised version received 30 January 2004

Available online 26 April 2004

Abstract

Dystrophin is a cytoskeletal protein normally expressed underneath the sarcolemma of muscle fibers. The lack of dystrophin in Duchenne muscular Dystrophy (DMD) muscles results in fiber necrosis, which was proposed to be mediated by chronic calcium mishandling. The extensive comparison of dystrophic cells from human or *mdx* mice with normal muscles have suggested that the lack of dystrophin may alter the resting calcium permeability and steady-state levels of calcium, but this latter observation remains controversial. It is also not clear, whether calcium mishandling is resulting from the dystrophic process or if dystrophin can directly regulate calcium handling in muscle cells. This prompted us to determine if transfection of full-length dystrophin or Becker Muscular Dystrophy (BMD) minidystrophin, a candidate for viral-mediated gene therapy, could change calcium handling properties. We took advantage of specific properties of Sol8 cell line showing the absence of dystrophin expression together with a drastic calcium mishandling. Here, we show that full-length dystrophin allowed the recovery of a low resting intracellular-free calcium concentration together with lower calcium transients. We also show for the first time that stable expression of minidystrophin was able to restore normal calcium handling in Sol8 myotubes through a better control of steady-state levels, calcium transients, and subcellular calcium events. It suggests that dystrophin could play a regulatory role on calcium homeostasis apparatus and that functional links exist between calcium signaling and cytoskeleton.

Keywords: Calcium homeostasis; Calcium release; DMD; Dystrophin; Minidystrophin; Sol8 cell line

Introduction

Dystrophin is a 427-kDa cytoskeletal protein normally expressed at the inner face of the sarcolemma of muscle fibers [1], where it associates with a large complex of proteins known as the dystrophin-associated proteins (DAPs) that includes dystroglycans, sarcoglycans, syntrophins, dystrobrevins, and sarcospan [2]. At this site, dystrophin links the internal cytoskeleton network to the extracellular matrix via the DAPs complex [3,4]. The lack of dystrophin in dystrophic muscle results in loss of all the DAPs with the disruption of this connexion, and finally, in muscle fiber necrosis. The complete function of dystrophin protein in skeletal muscle has not yet been fully elucidated, although it is thought to provide a crucial link between the intracellular actin-based cytoskeleton and the extracellular matrix [5]. The full-length 427 kDa dystrophin protein consists of four main structural domain. These include an NH_2-terminal actin binding domain, a central rod domain consisting of 4 hinge regions and 24 units with homology to those in β-spectrin, a cystein-rich domain, and a COOH-terminal domain both involved in linkage with DAPs. Mutations of the dystrophin gene lead to Duchenne muscular dystrophy (DMD) or the milder Becker muscular dys-

* Corresponding author. Lab des Biomembranes et Signalisation Cellulaire, Institut de Physiologie et Biologie Cellulaire, UMR CNRS 6558, Université de Poitiers 6187, Pôle Biologie Santé, 40 Avenue du Recteur Pineau, 86022 Poitiers cedex, France. Fax: +33-5-49-45-40-14.
E-mail address: bruno.constantin@univ-poitiers.fr (B. Constantin).

0014-4827/$ - see front matter © 2004 Elsevier Inc. All rights reserved.
doi:10.1016/j.yexcr.2004.02.032

trophy (BMD) which is associated with the expression of a truncated 229 kDa protein lacking 17 units in the central rod domain [6]. A 6.3-kb minidystrophin cDNA has been cloned from an asymptomatic BMD patient [7]. Its size is sufficiently small to be accommodated by current retroviral vector systems and it has been successfully expressed in vivo with accumulation of the minidystrophin at the sarcolemma and functional recovery in *mdx* mice [8–10].

The extensive study of DMD in human and animal models has also suggested that an alteration of calcium homeostasis occurs in dystrophic cells. It was first proposed that the cell necrosis process resulted from activation of protein degradation by elevated free calcium levels [11], a hypothesis supported by several early observations reporting an elevation in total calcium content [12–15]. Several evidences have supported the idea of an alteration of calcium homeostasis in dystrophic cells including increased transarcolemmal calcium influx [16,17], increased permeability to divalent cations that enter through channel-blocker sensitive pathways [18,19], and entry of calcium via non-specific cationic channels. These include nicotinic receptor channels, mechano-sensitive cationic channels, or store-operated cationic channels and Transient Receptor Potential channels (TRPc) since such ionic channels have been shown to be more active in the membrane of dystrophic skeletal muscle cells [20–23]. Finally, several studies reported an elevation of the resting $[Ca^{2+}]_i$ in dystrophic cells but this feature remains controversial. While some observations reported resting $[Ca^{2+}]_i$ elevation in *mdx* myotubes and myofibers [18,24,25], other groups did not confirm this elevation in resting cytosolic calcium handling [26–28]. Different observations obtained in our group suggested that the elevation of the resting $[Ca^{2+}]_i$ could be dependent on differentiation stage in culture. While human DMD myotubes in primary culture did not develop a significant $[Ca^{2+}]_i$ increase [28,29], well-differentiated and contractile cocultured human DMD myotubes displayed calcium-handling alterations [17,30]. More recently, the use of recombinant aequorin have permitted to show a relation between the absence of dystrophin and an alteration in function of intracellular compartments involved in calcium handling, like mitochondria and the sarcoplasmic reticulum. Robert et al. [31] observed that upon stimulation, the Ca^{2+} responses in *mdx* myotubes was first augmented in mitochondria, and was only observed in the cytosol after 11 days of culture. This suggests that the elevation of resting cytosolic $[Ca^{2+}]_i$ appears sequentially after subcellular alteration in calcium-buffering organelles.

These comparisons between dystrophic and control muscle cells suggest that dystrophin plays a regulatory role on calcium handling and transsarcolemmal calcium transport in normal skeletal muscle cells, and that alterations of calcium homeostasis could be directly the result of the lack of this regulatory protein. Alternatively, calcium mishandling could occur very indirectly during the degeneration process of dystrophic cells and dystrophin could play no primary control on calcium signalling proteins. One could address this question more directly by introducing the recombinant protein into dystrophin-deficient muscle cells displaying major calcium abnormalities and by observing relatively rapid changes in calcium handling and signalling properties. A previous study from McCarter et al. [32] have shown that lipofection of full-length dystrophin in *mdx* myotubes was lowering the resting $[Ca^{2+}]_i$ and the activity at rest of calcium leak channels responsible of calcium influx.

In this study, we took advantage of some characteristics of Sol8 myotubes, namely the lack of dystrophin [33] and a clear increase in $[Ca^{2+}]_i$ at the later stages of the development on the contrary of normal primary cultures [34]. Full-length dystrophin was transfected by microinjection into myotubes to explore the consequences on $[Ca^{2+}]_i$ but also on intracellular calcium-release processes, the main source of calcium ions during the triggering of contraction. Indeed, our previous work suggested that calcium mishandling in human DMD myotubes was also associated with increased spontaneous or depolarisation-induced calcium transients [30,35]. Since, the BMD minidystrophin was reported to mimic some of the functions of the 427 kDa dystrophin, we also explored the abilities of the truncated protein to regulate the resting $[Ca^{2+}]_i$ and the calcium-release process. The inclusion of the cDNA in a retroviral vector allowed us to obtain stable clones of myoblast constitutively expressing the BMD minidystrophin. We thus further explored the cell sorting of some DAPs and the subcellular pattern of spontaneous calcium-release events by fluorescence confocal microscopy.

Materials and methods

Cell culture

Experiments were performed on a dystrophin and calcium handling-deficient Sol8 subline [34] that derives from the original Sol8 myogenic cell line previously established from primary culture of normal C3H mouse soleus muscle [36]. Cells were seeded on glass coverslips in 35-mm plastic dishes (Greiner, Frickenhausen, Germany; 2 ml/dish). Myoblasts were grown in: Dulbecco's modified Eagle medium (DMEM, Cambrex, Verviers, Belgique) supplemented with 10% fetal calf serum (Biowest, France), 1% L-glutamine (Invitrogen, Cergy-Pontoise, France) and 1% antibiotics (penicillin-G, 100 i.u./ml, and streptomycin, 100 μg/ml; Invitrogen,). Following 2–3 days of proliferation (37 °C, 5% CO_2, water-saturated air) to around 80% of confluence, the growth medium was replaced by a differentiation medium (DMEM supplemented with 2% heat-inactivated horse serum (Invitrogen), 10 μg/ml insulin (Sigma), 1% L-glutamine and 1% antibiotics) to promote fusion of myoblasts into myotubes. For primary cultures, mouse satellite cells were isolated from hindlimb muscles of 3- to 5-week-old female mice killed by ether asphyxia. Muscles were minced and washed in a calcium- and magnesium-free medium (PBS medium containing: 140 mM NaCl; 2.7 mM

KCl; 1.8 mM KH_2PO4; 10 mM Na_2HPO_4; 37°C) and then transferred in a solution containing HamF-12 medium (Cambrex,) with 1.5 mg/ml collagenase I (Sigma, St. Louis, MO), 2 mg/ml protease IX (Sigma), 2 mM HEPES for dissociation (45 min, 37°C) with continuous stirring. The supernatants were centrifuged (20 min at room temperature, 350 × *g*) and the pellets were resuspended in a growth medium DMEM, supplemented with 10% fetal calf serum and 10% heat-inactive horse serum. The cell suspension was then filtered on a nylon netting (pore size 21 μm) in culture flasks and preplated in 100 mm plastic Petri dishes for an hour (37°C, 5% CO_2, water-saturated air) to remove most of the adhering non-muscle cells. Then cells were seeded in 25 cm^2 culture flasks and again incubated in same conditions. After 3 days, the cells were detached from the flasks by trypsin solution (trypsin and EDTA in Ca^{2+}- and Mg^{2+}-free HBSS, Invitrogen) and plated on gelatin-coated glass coverslips in 35-mm plastic dishes. The next day, the growth medium was exchanged for a fusion medium: DMEM supplemented with 5% heat-inactivated horse serum. All culture media contained penicillin-G (100 U/ml), streptomycin (100 μg/ml) and L-glutamine (2 mM).

Expression of dystrophins

Microinjection of Sol8 myotubes with full-length dystrophin cDNA

Expression of dystrophin in Sol8 myotubes was performed by microinjection of a plasmid expression vector (pTG11025, Transgene S.A., Strasbourg, France) encoding for the full-length human dystrophin. Cells were injected 2 days after promoting fusion (F+2) using an Eppendorf system coupled with an inverted microscope (Olympus, Tokyo, Japan). Plasmid pTG11025 cDNA was co-injected with the PEGFP-C1 plasmid (Clontech, Palo Alto, CA, USA) coding for the green fluorescent protein (EGFP) to find back transfected cells from green fluorescence. Glass needles (200–400 KΩ) were stretched with a vertical puller (Kopf Instruments, Tujunga, CA, USA). Usually 20 to 30 myotubes were microinjected in each culture dish. After microinjection, cells were rinsed twice and incubated at 37°C in differentiation medium.

Retrovirus infection of myoblasts with minidystrophin cDNA

The control cell line SolC1 is a mock-transfected subclone of Sol8 cell line that was retained for its ability to form numerous myotubes and obtained after transfection with an empty expression vector and a G418 selection. Transfection of minidystrophin was performed by two cycles of incubation of Sol8 myoblasts with the culture supernatant of E17 cells (10 times concentrated) producing the retrovirus RVTG 5251 (Clone 5251–86, Transgene S.A., manuscript in preparation). For isolation of stable clones, cells were trypsinized 48 h after transfection and plated at clonal density (6 cells/cm^2). The selection of the resistant colonies was performed by adding 1 to 1.5 mg of the neomycin analogue G-418 (Life Technologies). Resistant clones were analyzed for minidystrophin expression by Western blotting and immunological staining, and the colonies showing highest levels of minidystrophin expression were subcloned. After cloning, two selected subclones, named SolD6 and SolD7, were cultured like Sol8 and SolC1 dystrophin-deficient cells as described above.

Immunological staining

Dystrophin, dystrophin-associated proteins, and utrophin labelling were performed by indirect immunofluorescence using primary monoclonal mouse or polyclonal rabbit antibodies. We used monoclonal antibodies (Novocastra Laboratory, Newcastle upon Tyne, UK) raised against the C-terminal domain of dystrophin (NCL-DYS2), α-sarcoglycan (NCL-α-SG), β-dystroglycan (NCL-β-DG), γ-sarcoglycan (NCL-γ-SG), a polyclonal antibody against rod portion of utrophin (gift from Prof. M. Schaub, University of Zürich, Switzerland) and polyclonal antibodies (gifts from Dr S.C. Froehner, University of North Carolina, USA) against α_1-syntrophin (SYN17), α-dystrobrevin-1 (αDB638), and α-dystrobrevin-2 (αDB2). All these monoclonal [37,38] or polyclonal [39,40] antibodies have been previously tested in mouse muscle cells. Calcium transport proteins were immunolabelled using monoclonal antibody against the SERCA1 isoform of the sarcoplasmic reticulum Ca^{2+}-ATPase (a gift from Dr. E. Kordeli, University of Paris VII, France), monoclonal antibody against the ryanodine receptor (SIGMA, L'Isle d'Abeau Chesnes, France), and monoclonal antibody against the α_1-subunit of the dihydropyridine receptor (Affinity BioReagents, Golden, CO, USA). Myofilaments were visualized by using a monoclonal antibody against troponin-T (Sigma).

The cultured cells were fixed in TBS/4% paraformaldehyde and permeabilized with TBS/0.5% Triton X-100. Samples were then incubated for 1 h with primary antibodies in TBS (20 mM Tris base, 154 mM NaCl, 2 mM EGTA, 2 mM $MgCl_2$, pH 7.5)/1% BSA (Sigma). After washing in TBS, the cells were incubated for 30 min in TBS/1% BSA with Cy3-conjugated goat anti-mouse or anti-rabbit secondary antibodies (Jackson Immunoresearch, West Grove, PA, USA). Samples were mounted using Vectashield mounting medium (Vector, Burlingame, CA, USA). Nuclei were stained in the far red with TO-PRO-3 dye (Molecular Probes, Eugene, OR, USA).

Cytofluorescence analysis by confocal laser-scanning microscopy (CLSM)

The immunolabelled samples were examined by confocal laser-scanning microscopy (CLSM) using a Bio-Rad MRC 1024 ES (Bio-Rad, Hemel Hempstead, UK) equipped with an argon-krypton gas laser. The Cy3 fluorochrome was excited with the 568-nm yellow line and the emission was collected via a photomultiplier through a 585-nm long pass

filter. Data were acquired using an inverted microscope (Olympus IX70) and processed with the LaserSharp software (version 3.0, Bio-Rad). The images were performed at equal excitation parameters.

Intracellular-free calcium concentration measurements

Intracellular-free calcium measurements were performed with a ratiometric fluorescence method using an OSP100 microscopic photometry system (Olympus) and the calcium fluorescent probe Indo-1. The ratiometric method and the calibration procedure have been published elsewhere [41,42]. The ratio (R) of the dual emission fluorescence of the free and Ca^{2+}-bound forms of Indo-1 (at 485 and 405 nm, respectively) were separated, filtered, and collected by two photomultipliers. The intracellular-free calcium concentrations were calculated from the following equation [41]: $[Ca^{2+}]_i = Kd \times \beta \times [(R - R_{min}) / (R_{max} - R)]$. All the experiments were performed at room temperature.

Briefly, cells were rinsed twice with control solution (130 mM NaCl, 5.4 mM KCl, 2.5 mM $CaCl_2$, 0.8 mM $MgCl_2$, 5.6 mM glucose, 10 mM HEPES, pH 7.4), incubated for 45 min at room temperature in the same solution supplemented with 3 μM (final concentration) of the acetoxy-methyl ester form of Indo-1 (Indo-1/AM, Sigma). After loading, cells were washed with the control solution and incubated 15 min at 37°C to obtain complete de-esterification of the probe. Intracellular-free calcium measurements were performed in control solution. For evaluation of the calcium transients during depolarizing stimulation, a 100-mM KCl solution was made from control solution by replacement of 130 mM NaCl by 35 mM NaCl + 95 mM KCl. The solution was applied in the neighbourhood of the interrogated cells with a homemade gravity microperfusion device, until peak level reached its maximum.

Imaging of intracellular-free calcium concentration by CSLM

Calcium signals were recorded using a confocal microscopy system and Fluo-4 as fluorescent probe. Cells were loaded with 3 μM fluo-4 acetoxymethyl (AM) ester (Sigma) for 10 min at room temperature in PBS solution, rinsed and allowed to equilibrate for 10 min more to complete de-esterification of dye by intracellular esterases. The fluorescence of Fluo-4-loaded cells was detected with a Biorad MRC 1024 equipped with a 15-mW argon-krypton gas laser. The confocal unit was attached to an inverted microscope (Olympus IX70) with a 60× water immersion objective. The Fluo-4 fluorochrome was excited with the 488-nm blue line and emission of the dye was collected via a photomultiplier through a 522-nm pass band filter. Two dimensional images composed of 256 × 256 pixels (8 bits/pixel) were acquired every 300 ms. Graphic representations are obtained by integrating defined zones and give temporal evolution of row fluorescence in the different territories.

Electrophoresis and Western blot

Total protein extracts from SolD7 and SolC1 cultured myotubes were obtained by lysing cells into a lysis buffer (100 mM NaCl, 50 mM Hepes, 20 mM EGTA, 1.5 mM $MgCl_2$, 10% glycerol, 1% Triton × 100, pH 7.5) supplemented with protease inhibitors (5 μg/ml Leupeptin, 1% Aprotinin, 0.5 mM PMSF; Sigma). Denatured protein samples were concentrated and separated by SDS-PAGE on 5% polyacrylamide gels (Boehringer Mannheim) for migration of dystrophin, minidystrophin and utrophin or on 12% polyacrylamide gels for migration of β-enolase, troponin-T and α-tubulin. Electrotransfer to nitrocellulose membrane (Bio-Rad) was performed overnight at 4°C using a wet-transfer apparatus (Mini-Protean II, Bio-Rad) and a voltage of 25 V. The blot was blocked for 4 h at 4°C in TBS/2% BSA and then incubated 3 h at 4°C with 1: 300 of the NCL-DYS2 primary antibody, or 1: 2000 of a polyclonal antibody against rod portion of utrophin (gift from Prof. M. Schaub, University of Zürich, Switzerland) diluted in TBS/1% BSA supplemented with 0.1% Tween 20. Other antibodies used for Western blot analysis were 1: 1000 monoclonal antibodies against troponin-T (Sigma), and 1: 5000 monoclonal antibody against α-tubulin (Sigma). After washing, the blot was treated for 1 h with 1: 5000 horse radish peroxydase conjugated anti-mouse antibodies or 1: 5000 horse radish peroxydase conjugated anti-rabbit antibodies (Amersham, Les Ulis, France), and developed with an ECL kit (Amersham). The apparent molecular weight of proteins was estimated according to the position on the blot of prestained protein markers (Bio-Rad).

Statistical analysis

Myotube $[Ca^{2+}]_i$ values are shown in nM and are reported as the mean ± SEM. Statistical significance was determined using a two-tailed Student's *t* test for unpaired data (GraphPad Prism 3.0, GraphPad Software, San Diego, CA, USA) and was considered significant when $P < 0.05$.

Results

Changes in intracellular-free calcium concentration during culture of dystrophin-deficient SolC1 subclones

We have previously shown that, on the contrary to normal rat primary cultures of myotubes, the intracellular-free calcium concentration ($[Ca^{2+}]_i$) was increasing in dystrophin-deficient Sol8 myotubes during the time of culture [34]. We also used the ratiometric methods with indo-1 loaded myotubes for evaluating resting $[Ca^{2+}]_i$ in the additional control SolC1 subclone. This dystrophin-deficient cells were developed as a mock-transfected cell line and obtained after transfection with an empty expres-

sion vector and selection by G418. Fig. 1 shows that SolC1 myotubes retained the properties of a spontaneous and abnormal increase in the resting $[Ca^{2+}]_i$. A drastic increase of 54 nM occurred between the differentiated stage F+3 (3 days after fusion potentiation) and F+4 (4 days after fusion). The resting-free calcium concentration further increase at F+5 stages (+20 nM to +40 nM depending of the culture), and then return at F+6 to levels of F+4 stages (between 130 and 140 nM). At these latter stages, remaining myotubes displayed intracellular vacuoles (Fig. 1 right bottom image) and numerous cells detached and died. Comparing to solC1 differentiated cells mouse myotubes in primary cultures (expressing native 427 kDa dystrophin) displayed a constant value of resting $[Ca^{2+}]_i$ maintained around 100 nM all along the duration of culture. Primary mouse myotubes can still grow and differentiate beyond F+6 stage.

Forced expression of dystrophins

Expression of full-length dystrophin in Sol8 myotubes

F+2 Sol8 myotubes were directly microinjected with a cDNA plasmid containing the full-length dystrophin gene. These microinjected myotubes were identified through the green fluorescence of the EGFP (Fig. 2a) and appeared morphologically similar to the non-injected ones. Approximately 15% to 25% of the EGFP-expressing myotubes also expressed dystrophin (Fig. 2b). As shown in Fig. 2b, when transfected with full-length dystrophin cDNA, Sol8 myotubes exhibited the expected sarcolemmal staining of dystrophin with NCL-DYS2 antibody, as shown by bright fluorescence. Functional experiments (see below) were done on the EGFP-positive myotubes. All the dystrophin-positive myotubes observed in the dystrophin immunostained cultures expressed EGFP, confirming that there was no endogenous dystrophin in Sol8 cells. Absence of 427 kDa dystrophin in non-microinjected Sol8 cells was also confirmed by immunofluorescence using NCL-DYS3 antibody (Novocastra Laboratory) directed against the N-terminus domain of dystrophin, and also by immunoblots using NCL-DYS2 antibody (not shown).

Expression of mini-dystrophin in SolD7 line

Immunological staining of dystrophin was performed on both age-matched SolC1 and SolD7 cultured myotubes (Figs. 2c, d). Examination by CLSM and immunostaining demonstrated the correct cortical distribution of BMD minidystrophin when expressed in differentiated SolD7 myotubes (Fig. 2d). Cloning of SolD7 cells resulted in a constitutive expression of the minidystrophin in nearly all SolD7 myoblasts and myotubes (Fig. 2e). The truncated dystrophin was never addressed at the sarcolemma in SolD7 myoblasts (Fig. 2e, upper panel) and the correct sorting was concomitant with terminal differentiation and correct sarco-

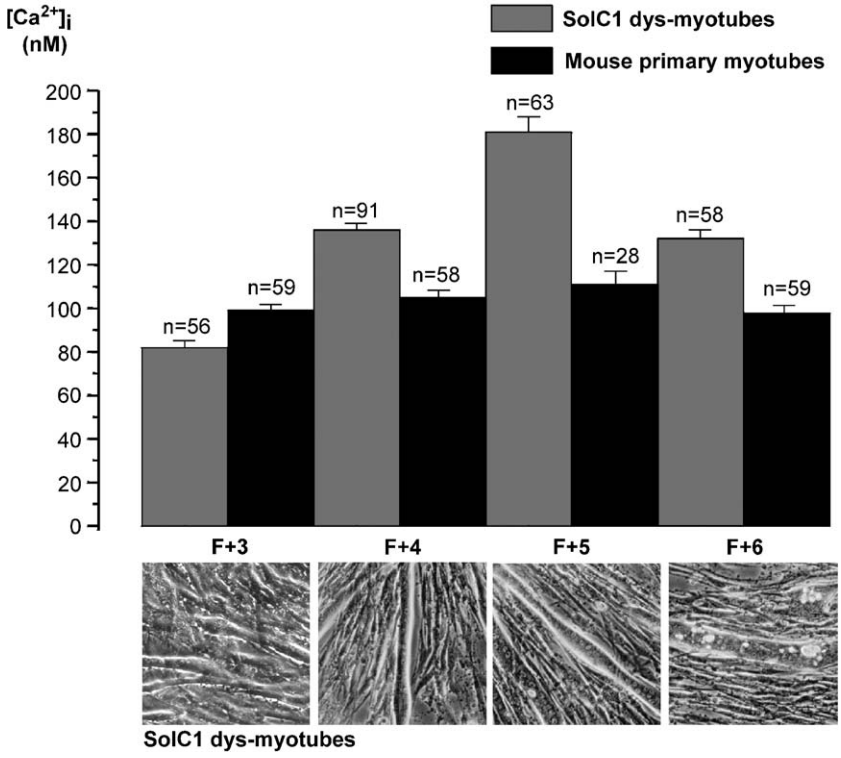

Fig. 1. Changes in resting $[Ca^{2+}]_i$ during culture of dystrophin-deficient SolC1 subline of myotubes and mouse myotubes from primary culture. Histogram of mean resting $[Ca^{2+}]_i$ evaluated by ratiometric photometry in indo-1 loaded myotubes at four different stages of culture after promotion of cell fusion: F+3, F+4, F+5 and F+6. Mean resting $[Ca^{2+}]_i$ were obtained from two different sets of experiments. Microphotographs under each column illustrate the typical appearance of SolC1 myotubes for each stage.

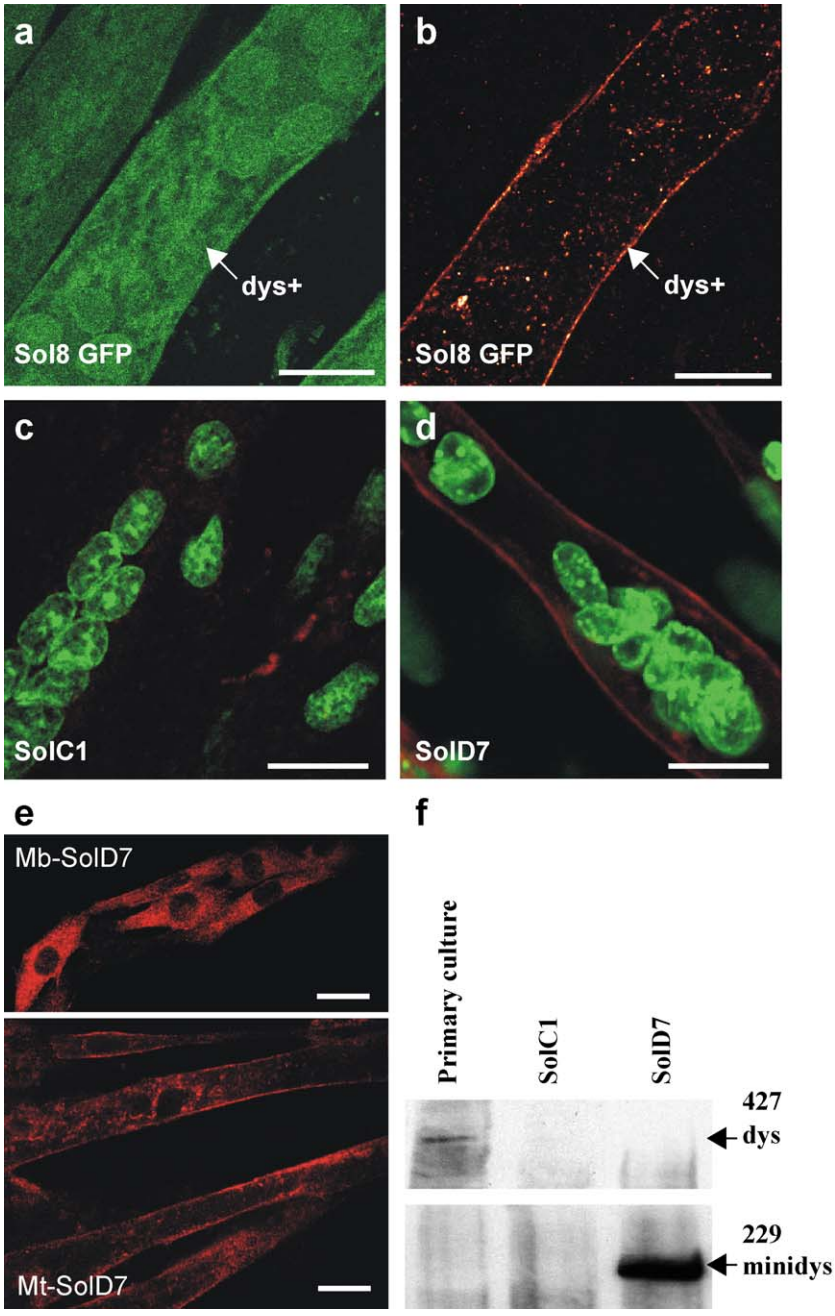

Fig. 2. Expression of dystrophin and minidystrophin after transfection of Sol8 myogenic cells. (a, b) EGFP (green channel, a) and dystrophin (red channel, b) detection in F+4 microinjected Sol8 myotubes observed by CLSM. Dystrophin expression was detected using NCL-DYS2 monoclonal antibody. (c, d) Examples of double immunofluorescence staining of dystrophin and nuclei in SolC1 control stable cell line (c) and in SolD7 myotube transduced with minidystrophin retrovirus (d). Scale bar, 20 μm. (e) Visualization of minidystrophin distribution in SolD7 clones at myoblast stage (upper panel), and after differentiation (lower panel). (f) Total cell lysates from primary cultures, SolC1 and transfected SolD7 myotubes were migrated in parallel and analyzed by Western blot for 427 kDa dystrophin and 229 kDa minidystrophin expression. Equal amounts of proteins extract were loaded in each lane. Apparent molecular weight of the band revealed in SolD7 lane was estimated as approximately 220 kDa.

lemmal localization of β-dystroglycan (see below, Figs. 3c, d). As expected, dystrophin immunostaining has never been observed in the mock-transfected SolC1 line (Fig. 2c), used as control.

Immunoblotting with the monoclonal antibody NCL-DYS2 in 4-day-old SolD7 (Fig. 2f) myotubes revealed the presence of a protein, with an electrophoretic mobility compatible with the molecular weight of the 229-kDa minidystrophin protein, and its absence from protein extracts of mock-transfected SolC1 myotubes and control primary cultures. The higher band corresponding to the 427-kDa dystrophin and visible in total protein extracts from primary cultures was absent in SolC1 and SolD7 myotubes. The weaker density of the 427-kDa dystrophin comparing to

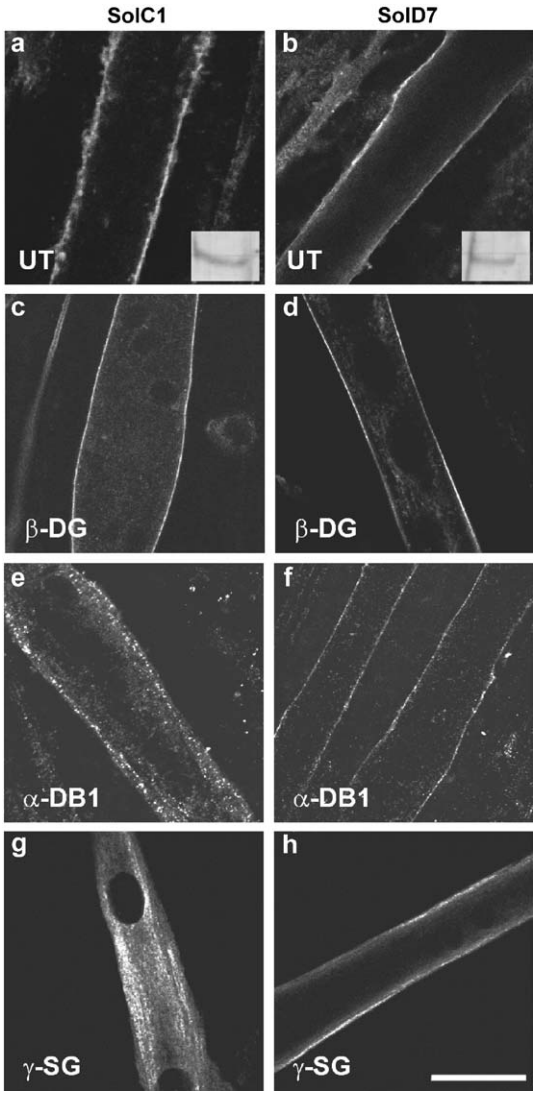

Fig. 3. Examples of subcellular localization of utrophin and members of the DAPs complex in F+4 control SolC1 myotubes (a, c, e, g), and F+4 SolD7 myotubes constitutively expressing the minidystrophin product (b, d, f, h). Fluorescence images were obtained after immunostaining by CLSM. UT: utrophin (a, b), β-DG: β-dystroglycan (c, d), α-DB1: α-dystrobrevin-1 (e, f), γ-SG: γ-sarcoglycan (g, h). Scale bar, 20 μm. Inset in a and b: Western blot analysis of utrophin expression in dystrophin-deficient SolC1 cells (a) and SolD7 myotubes expressing minidystrophin (b). Total cell lysates (20 μg of protein) were migrated in parallel and revealed after Western blotting with a polyclonal antibody against the central rod domain of utrophin.

the band of the BMD minidystrophin was not only due to the high expression level of the latter. The band of full-length dystrophin was also underestimated because of the presence in total protein lysates of proteins from undifferentiated myoblasts and from fibroblasts.

These results clearly confirm that a myogenic cell line expressing high amount of human minidystrophin was generated. The retroviral genome is stably integrated into host cell genomic DNA, since SolD7 cell line allows stable production of minidystrophin for at least 15 passages.

Expression of dystrophin-associated and -related proteins in SolC1 and SolD7 myotubes

We first examined if dystrophin-deficient and dystrophin-expressing myotubes were expressing the dystrophin-related protein utrophin. Immunostaining with a specific polyclonal antibody that do not cross-react with dystrophin revealed that utrophin was equally present at the sarcolemma of dystrophin-negative Sol8 (not shown) and SolC1 (Fig. 3a) myotubes and of minidystrophin-positive SolD7 myotubes (Fig. 3b). Western blot analysis showed that the levels of expression of utrophin (inset in Figs. 3a, b) are not significantly different in the two populations of myotube. Examination of the cellular localization of dystrophin-associated proteins was also performed in dystrophin-negative SolC1 myotubes (Figs. 3c, e, g) and minidystrophin-positive SolD7 myotubes (Figs. 3d, f, h) comparatively. As previously described in Sol8 myotubes [34], β-dystroglycan was correctly expressed and located at the sarcolemma (Fig. 3c) of SolC1 myotubes. This was of particular interest in the aim of forced dystrophin expression since β-dystroglycan links and anchors dystrophin at the inner face of the sarcolemma. Similarly to Sol8 myotubes, α-sarcoglycan was never expressed in SolC1 myotubes (not shown). However, α-dystrobrevin-2 (not shown) and α_1-syntrophin (not shown) were both normally located at the sarcolemma of SolC1 myotubes. β-dystroglycan (Fig. 3d), α-dystrobrevin-2 (not shown) and α_1-syntrophin (not shown) followed a similar detection pattern in age-matched SolD7 myotubes expressing minidystrophin.

Two dystrophin-associated proteins, the γ-sarcoglycan and the α-dystrobrevin-1, showed abnormal localization in SolC1 myotubes. Immunostaining of γ-sarcoglycan showed a fully cytoplasmic localization (Fig. 3g) and α-dystrobrevin-1 was cytoplasmic and mainly distributed at a subsarcolemmal area (Fig. 3e). In SolD7 myotubes, γ-sarcoglycan (Fig. 3h) and α-dystrobrevin-1 (Fig. 3f) were properly expressed at the sarcolemma membrane after minidystrophin expression.

This shows that forced expression of minidystrophin in cultured myotubes is able to reactivate appropriate sarcolemmal sorting of γ-sarcoglycan and α-dystrobrevin-1, two members of the DAPs complex.

Consequences of dystrophin expression on the dissociation constant (Kd) of the Ca^{2+} + Indo-1 reaction

Many authors have shown that the dissociation constant (Kd) affinity of the Ca^{2+} + Indo-1 reaction is affected by different factors, such as pH [43] or binding to cytosolic proteins [44,45]. We evaluated Kd in situ in both control SolC1 and minidystrophin-positive SolD7 myotubes, to take into account the minidystrophin concentration in SolD7 myotubes. Dye calibration in situ was performed following a procedure derived from Gailly et al. [26]. After loading with Indo-1/AM, cells were treated with 20 μg/ml α-toxin (Calbiochem, San Diego, CA, USA) for 20 min in calcium-

free medium. R_{min} was determined after 30 min incubation in the calcium-free medium. Then, cells were incubated 10 min in Ca-buffer solutions (135 mM NaCl, 10 mM EGTA, 1 mM $MgCl_2$, 5 mM glucose, 10 mM Hepes, pH 7.2) of increasing values of free Ca^{2+}. The Ca^{2+} + Indo-1 reaction has a Kd of 331 nM in minidystrophin-positive SolD7 myotubes, and 329 nM in control SolC1 myotubes, with a Hill's coefficient of 1.96 and 2.05, respectively (Fig. 4). These parameters were considered as the same in both SolD7 and SolC1 cells, justifying the use of a common Kd (330 nM) in computing $[Ca^{2+}]_i$.

Consequences of full-length dystrophin expression on calcium homeostasis

Consequences of full-length dystrophin expression on the resting $[Ca^{2+}]_i$ levels

Microinjected Sol8 myotubes expressing EGFP with or without recombinant full-length dystrophin were compared. Fig. 5 shows the mean (± SEM) values of the resting $[Ca^{2+}]_i$ levels in dystrophin-negative and in dystrophin-expressing myotubes at F+4 (Fig. 5a) and F+6 (Fig. 5b) stages. Full-length dystrophin-positive myotubes clearly showed a significant lower resting $[Ca^{2+}]_i$ level than dystrophin-negative myotubes at F+4 (109 ± 6 nM vs. 130 ± 3 nM, $P < 0.05$) and at F+6 stages (76 ± 5 nM vs. 151 ± 6 nM, $P < 0.0001$). Interestingly, dystrophin-negative Sol8 myotubes exhibited an expected increase of resting $[Ca^{2+}]_i$ from F+4 to F+6 (130 ± 3 vs. 151 ± 6, $P < 0.05$), whereas full-length dystrophin-positive myotubes exhibited a reverse evolution with a decrease of resting $[Ca^{2+}]_i$ from F+4 to F+6 (109 ± 6 vs. 76 ± 5, $P < 0.005$). In parallel to these experiments, resting $[Ca^{2+}]_i$ was measured in SolC1dys-myotubes to compare in the same conditions this value with the one obtained in Sol8/EGFP dys-myotubes. This set of measures showed that F+4 SolC1 myotubes exhibited resting calcium levels (129 nM ± 2, $n = 18$) similar to Sol8 myotubes when cultured parallely. This also suggests that EGFP expression in Sol8 myotubes do not interfere with indo-1 measurements.

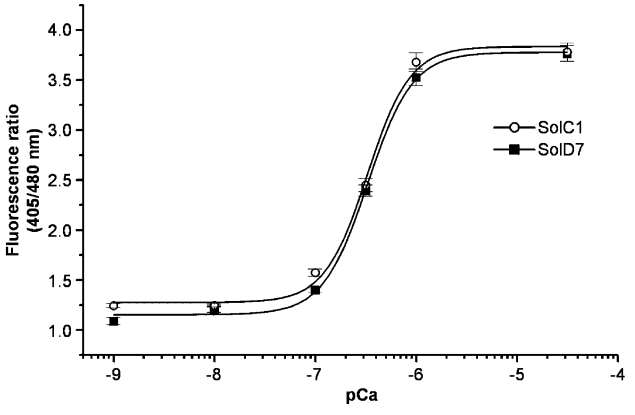

Fig. 4. In situ Kd determination of the Ca^{2+} + Indo-1 reaction. The 405/485 fluorescence ratio obtained in SolC1 (empty circles, $n = 11$) and SolD7 (full squares, $n = 12$) myotubes was plotted vs. cytosolic pCa and curves were fitted using a non-linear logistical equation (Origin 4.0, Microcal, Northampton, MA, USA). Scale bars indicate SEM.

Consequences of full-length dystrophin expression on the calcium transients during depolarizing stimulation

Measurements of $[Ca^{2+}]_i$ were performed during depolarizing stimulation by 100 mM KCl (Figs. 5c–e), in microinjected full-length dystrophin-positive Sol8 myotubes, as well as in their respective controls. Upon superfusion with 100 mM KCl, all the interrogated myotubes exhibited a dynamic response with a transient increase in $[Ca^{2+}]_i$.

Examples of 100 mM KCl-induced calcium transients obtained in microinjected F+4 Sol8 myotubes are presented in Fig. 5c. In EGFP-microinjected Sol8 myotubes, the mean of response amplitude variations was lower in full-length dystrophin-positive myotubes than in dystrophin-negative ones. The mean amplitude of calcium transients in dystrophin-expressing myotubes represented only 60% of the signal in dystrophin-negative cells at F+4 (Fig. 5d) and this difference was conserved at F+6 (Fig. 5e).

Consequences of BMD minidystrophin expression on calcium homeostasis

Consequences of BMD minidystrophin expression on the resting $[Ca^{2+}]_i$ levels

Measurements of resting $[Ca^{2+}]_i$ have been performed with indo1 probe in mock-transfected SolC1 and in minidystrophin-transfected SolD7 myotubes (Fig. 6a). At F+4 stage, resting $[Ca^{2+}]_i$ in SolD7 myotubes was significantly lower than in SolC1 myotubes (115 ± 2 nM vs. 145 ± 2 nM, $P < 0.01$). This difference was more pronounced at F+5 stage since the resting $[Ca^{2+}]_i$ was increased in SolC1 myotubes at a level of 160 ± 5 nM, while resting $[Ca^{2+}]_i$ levels remained at a stable mean value of 115 ± 2 nM in SolD7 myotubes. The resting $[Ca^{2+}]_i$ of SolD7 myotubes at F+4 and F+5 stages (115 nM) was closer to the levels observed in primary cultures (105 and 111 nM; Fig. 1). At F+6 stages, resting $[Ca^{2+}]_i$ was not significantly different (146 ± 4 nM vs. 145 ± 4 nM). SolD7 myotubes showed significant increase of their resting $[Ca^{2+}]_i$ level from F+4 to F+6 (115 ± 2 vs. 146 ± 4, $P < 0.0001$). This suggests that additional defects appears in SolD7 cells at F+6 days and are not corrected by minidystrophin. At this terminal stage, many SolC1 myotubes are dying and detaching which may explained that the resting $[Ca^{2+}]_i$ level is underestimated at F+6 vs. F+5 (145 ± 4 vs. 160 ± 5 nM, $P < 0.05$).

Consequences of BMD minidystrophin expression on the calcium transients during depolarizing stimulation

Measurements of $[Ca^{2+}]_i$ were performed during depolarizing stimulation by 100 mM KCl (Fig. 6b), in both microinjected, full-length dystrophin-positive Sol8 myotubes and minidystrophin-positive SolD7, as well as in their respective controls SolC1. The mean variation in response

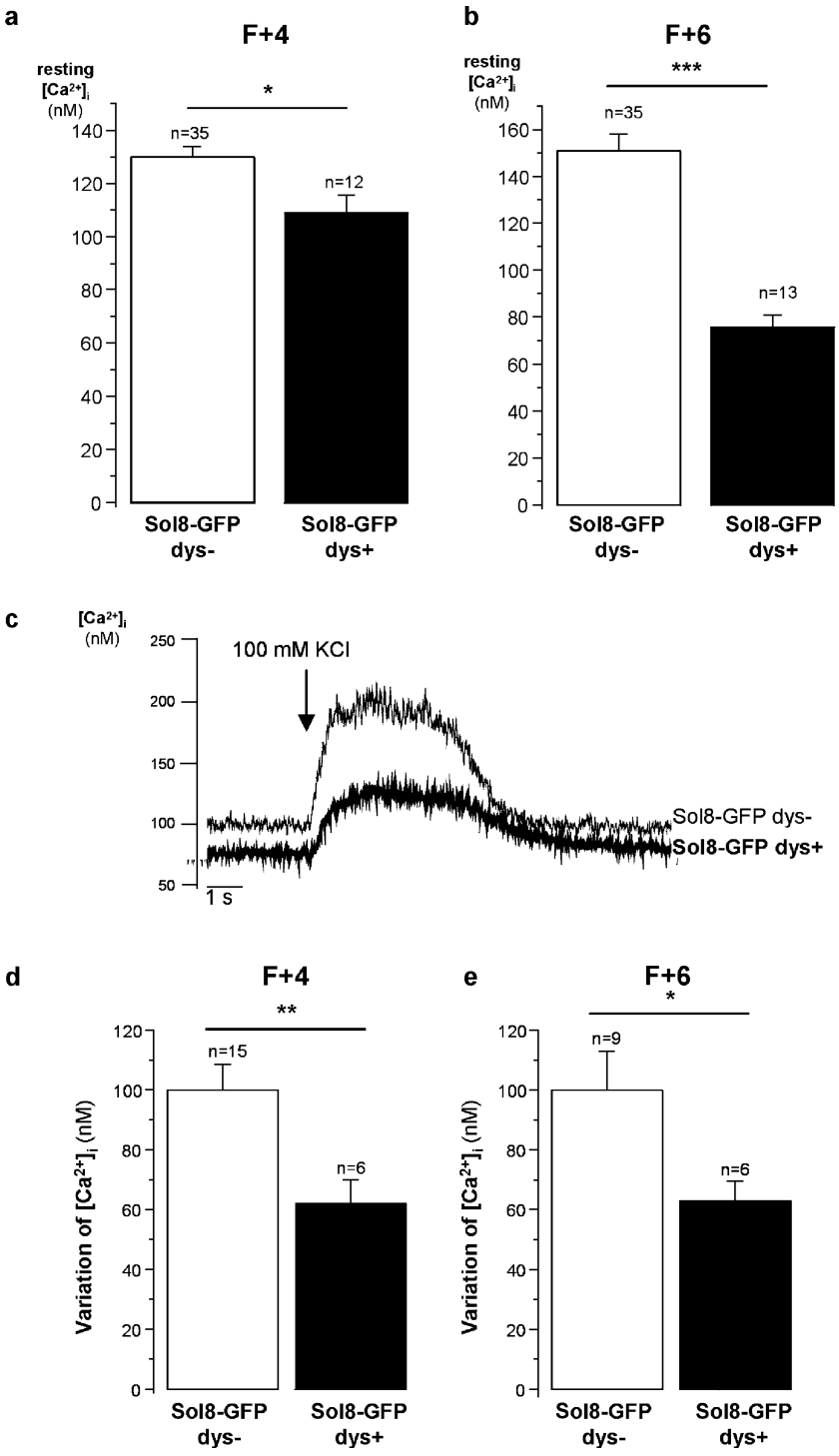

Fig. 5. Indo-1 ratiometric measurements of intracellular-free calcium concentration ($[Ca^{2+}]_i$) in dystrophin-negative (Sol8 dys−) and full-length dystrophin-positive (Sol8 dys+) microinjected Sol8 myotubes. Measurements were obtained at 4 (a) and 6 days (b) after promoting fusion. Each bar graph corresponds to the mean value of resting $[Ca^{2+}]_i \pm$ SEM (in nM). *n* above each bar graph indicates the number of tested cells. ns, non-significantly different; $*P < 0.05$; $**P < 0.01$; $***P < 0.0001$ (Student's unpaired *t* test). (c) Examples of Indo-1 ratiometric measurements of 100 mM KCl-induced calcium transients performed in dystrophin-negative (Sol8 dys−; thin trace) and full-length dystrophin-positive (Sol8 dys+; bold trace) microinjected F+4 Sol8 myotubes. (d, e) Histograms of response amplitude variations upon superfusion with 100 mM KCl in dystrophin-negative (Sol8 dys−) and full-length dystrophin-positive (Sol8 dys+) microinjected Sol8 myotubes. Each bar graph corresponds to the mean value of $\Delta\ [Ca^{2+}]_i \pm$ SEM (in nM) measured at 4 (d) and 6 days (e) after promoting fusion.

amplitude was lower in minidystrophin-positive SolD7 myotubes compared to control SolC1 myotubes. At F+4, the average amplitudes in minidystrophin cells represented 80% (Fig. 6b) of the average signal obtained in mock-transfected myotubes and only 60% at F+6 stages (Fig. 6c). Lower amplitudes of calcium transients in SolD7 myotubes

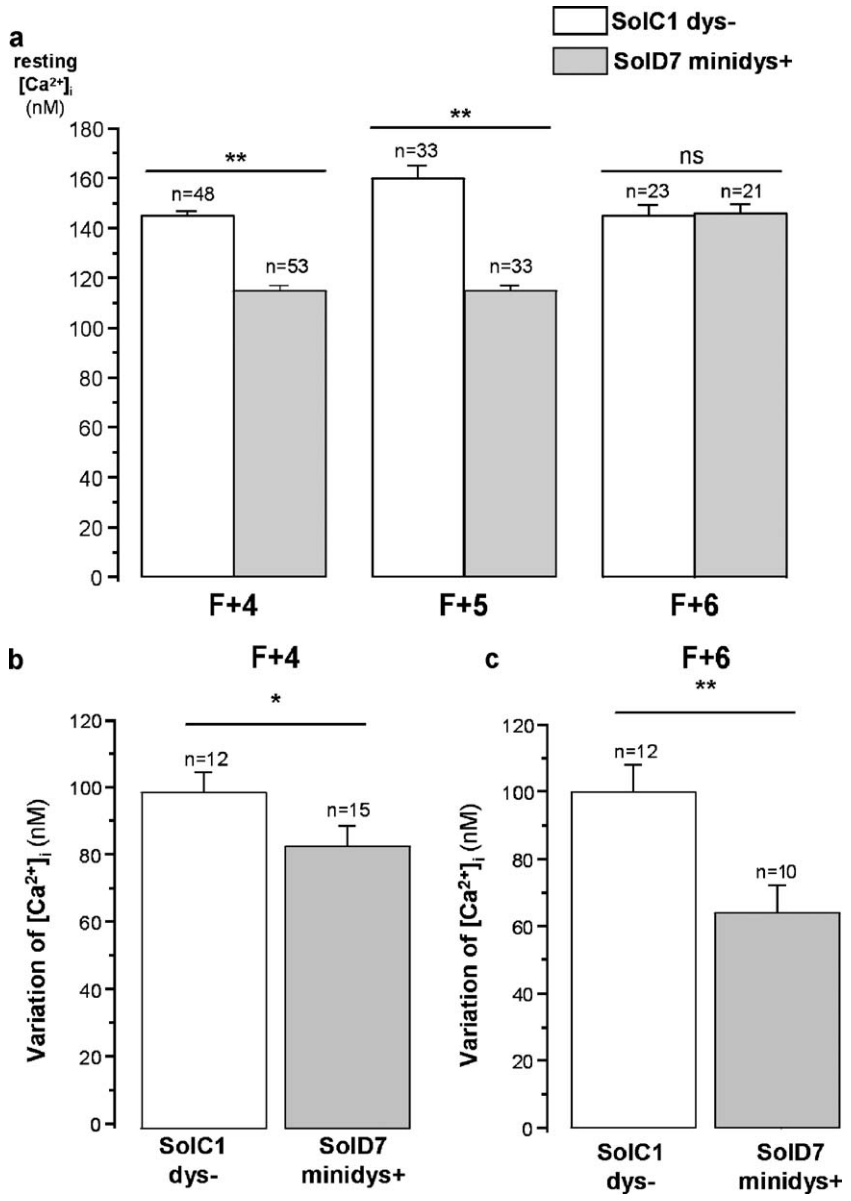

Fig. 6. Indo-1 ratiometric measurements of intracellular-free calcium concentration ($[Ca^{2+}]_i$) in control SolC1 and in minidystrophin-positive SolD7 myotubes. (a) Each bar graph corresponds to the mean value of resting $[Ca^{2+}]_i \pm$ SEM (in nM), measured in SolC1 (open box) and SolD7 (grey box), at 4, 5, and 6 days after promoting fusion. (b, c) Histograms of response amplitude variations upon superfusion with 100 mM KCl in control SolC1 (open box) and in minidystrophin-positive SolD7 (grey box) myotubes. Measurements were performed at F+4 (b) and F+6 (c) stages. Each bar graph corresponds to the mean value of response amplitude variations $\pm$ standard error (in nM). *n* above each bar graph indicates the number of tested cells. ns, non-significantly different; $*P < 0.05$; $**P < 0.01$ (Student's unpaired *t* test).

were closer to the mean amplitudes recorded in primary cultures of mouse myotubes (not shown).

In conclusion, expression of full-length dystrophin or BMD minidystrophin induced changes in calcium signaling properties that reduced the amplitude of calcium transients during depolarization of differentiated myotubes.

Consequences of minidystrophin expression on the spontaneous calcium-release activity

Since minidystrophin expression modified the calcium-release properties, we explored the spontaneous calcium-release events by CLSM on fluo4-loaded myotubes. Because emission of fluo4 is in the same wavelength range than EGFP, these events could not be analyzed on EGFP-injected Sol8 myotubes. We thus compared only the dystrophin-deficient SolC1 clones with the minidystrophin-expressing SolD7 cells. Both population of myotubes exhibited spontaneous intracellular calcium events. However, the dynamic and spatial pattern of calcium release and uptake in the two populations of cells were obviously different. As shown in Fig. 7, both populations of myotubes exhibited a basal and space-restricted activity of calcium release, which appeared

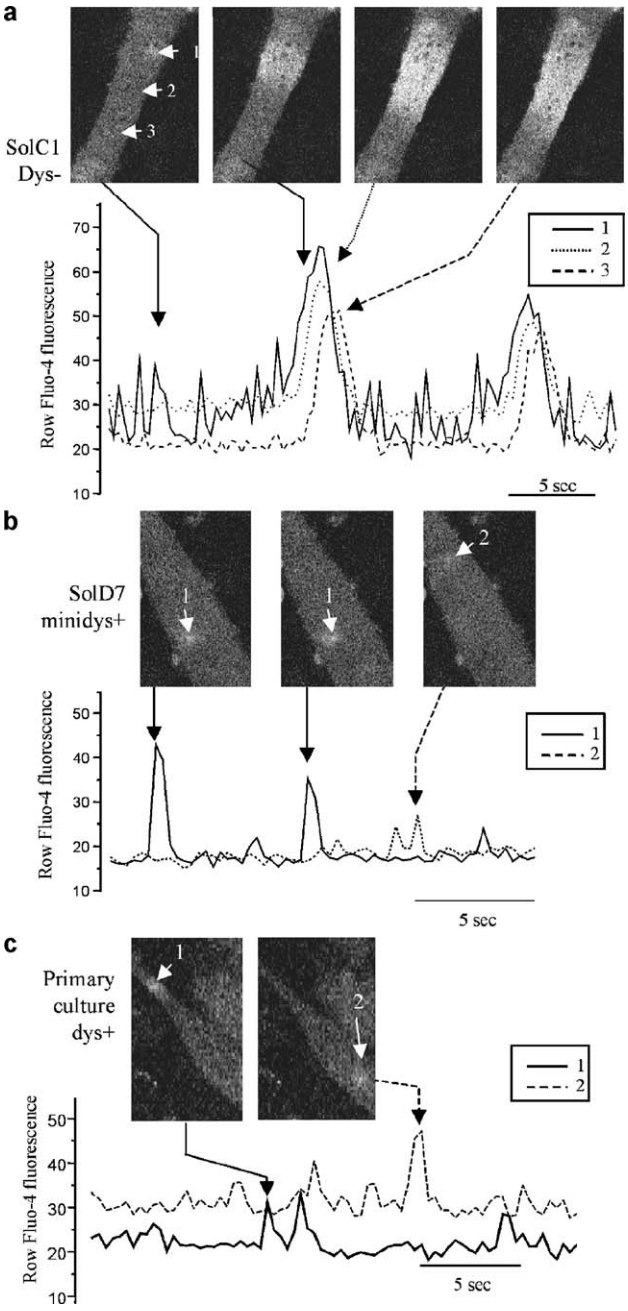

Fig. 7. Subcellular pattern of spontaneous calcium release in dystrophin-deficient myotubes (a) in minidystrophin-expressing myotubes (b) and in mice myotubes from primary culture (c), expressing native 427 kDa dystrophin. Two-dimensional images of Ca^{2+} release events in Fluo 4-loaded myotubes acquired by CLSM at a rate of 1 image every 300 ms. The time courses of fluorescence intensity (lower panels) measured at different areas of interest (white arrows on images) are shown for each set of images (upper panels).

in x/y longitudinal images as small fluorescent spots (Fig. 7a, left high panel; Fig. 7b, three high panels). This restricted spontaneous activity, corresponding to intracellular sparks, remained discrete and repetitive in all minidystrophin-expressing myotubes (SolD7, Fig. 7b). On the contrary, in 21% of dystrophin-deficient myotubes, spontaneous activity appeared less tightly regulated. In addition to space-restricted activities, Sol8 (not shown) and SolC1 myotubes often displayed calcium events with higher magnitude and a larger propagation in space (Fig. 7a). These propagating activities were extending to a large portion of myotubes as calcium waves (Fig. 7a, three right panels) in 6% of the cells presenting an activity. Sol8 myotubes expressing the minidystrophin (SolD7, Fig. 7b) developed an activity more similar to mouse myotubes from primary culture. These types of cells expressing native dystrophin exclusively displayed rare spontaneous calcium events with the characteristics of space-restricted calcium sparks (Fig. 7c).

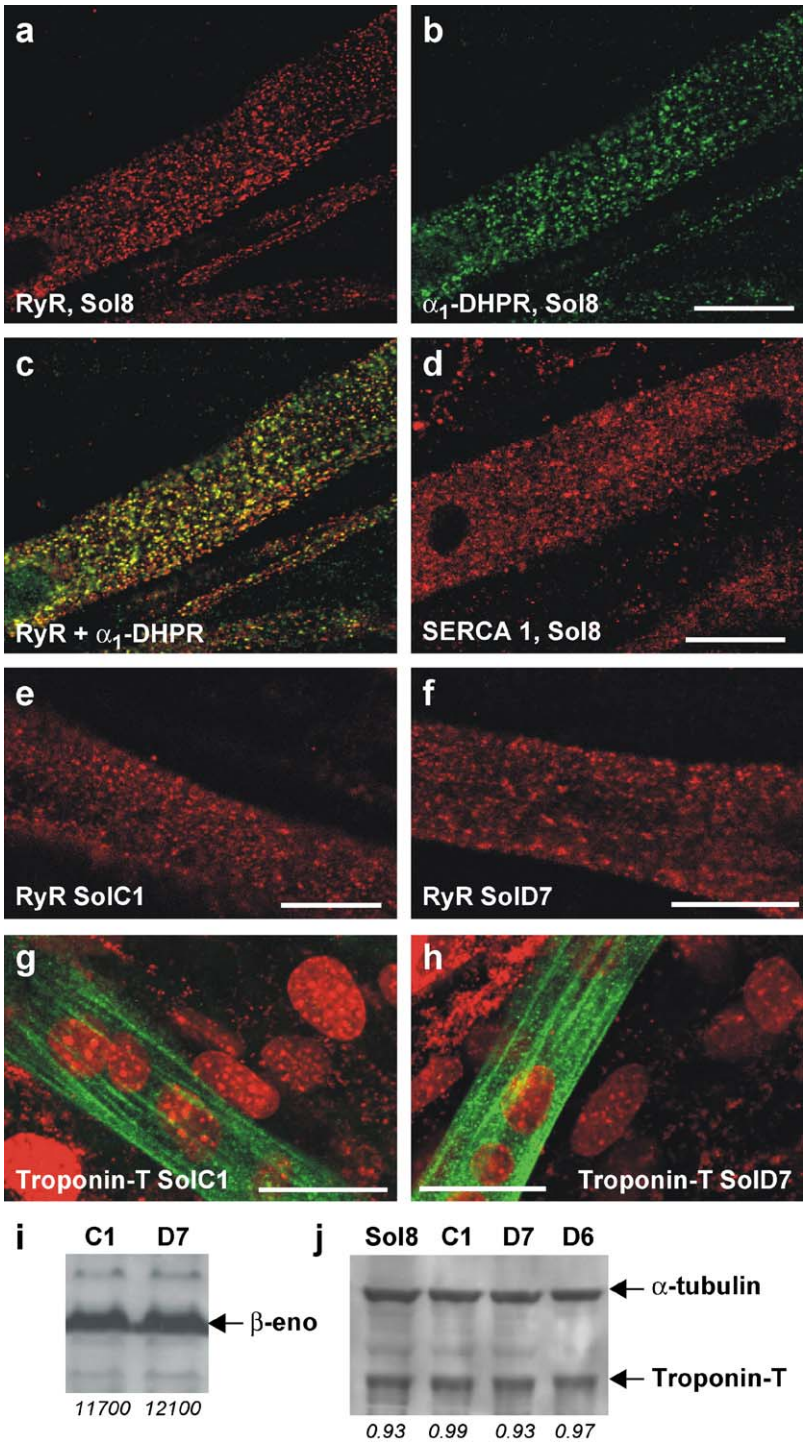

Fig. 8. Examples of immunostaining of calcium transport and sarcomeric proteins in differentiated myotubes (a–h), and Western blot analysis of differentiation markers β-enolase (i) and troponin-T (j). The ryanodine receptor (RyR), (a, red channel) and the α_1-subunit of the dihydropyridine receptor (α_1-DHPR) (b, green channel) were detected in the same F+4 Sol8 myotube by double staining with a rabbit polyclonal antibody and a mouse monoclonal antibody respectively. The merged image is shown in c, and colocalized vesicles appear in yellow. The sarcoplasmic reticulum Ca^{2+}-ATPase (SERCA-1) was also immunostained (d, red channel) as described in Materials and methods. Comparison of subcellular distribution of RyR in dystrophin-deficient SolC1 myotubes (e) and in SolD7 myotubes expressing minidystrophin (f). (g, h) Myofilaments were labeled by immunostaining using a monoclonal antibody recognizing troponin-T (green channel) into SolC1 myotubes (g) and SolD7 myotubes (h). Nuclei were stained in the same time using the DNA probe TO-PRO-3 (g, h, red channel). (i, j) Total cell lysates (20 μg of protein) were migrated in parallel and revealed after Western blotting with a polyclonal antibody against the β-enolase (i) or sequentially with monoclonal antibodies against troponin-T (j, lower bands) and against α-tubulin (j, upper bands). Results of densitometric analysis are shown under Western blot, as absolute values or ratio of troponin-T/α-tubulin. Cell lysates were obtained from age-matched Sol8 (Sol8), SolC1 (C1), and SolD7 (D7) myotubes. D6 column shows cell lysates from a second clone, SolD6, expressing mini-dystrophin like SolD7. Scale bar, 20 μm.

Subcellular distribution of calcium channels and pump

The differences in subcellular pattern of calcium signals could be due to changes in the organization of calcium release and calcium uptake sites. We thus explored the distribution of the intracellular transporters with immunostaining and CLSM analysis. In cultured dystrophin-deficient myotubes, calcium channels of the transverse tubules (dihydropyridine receptors, DHPR) and calcium channels of the sarcoplasmic reticulum (ryanodine receptors, RYR) appeared randomly distributed (Figs. 8a, b) without any alignment on transversal sarcomerization like in fibers. Numerous clusters of both channels were co distributed showing the abundance of coupling sites (Fig. 8c) also randomly dispatched throughout the myotubes. The Ca^{2+}-ATPase of the sarcoplasmic reticulum was displaying a similar punctuate pattern in the cytoplasm of myotubes without any sarcomerization in our culture conditions (Fig. 8d). The same distribution of ryanodine receptors was observed in minidystrophin-expressing myotubes (Fig. 8f) than in SolC1 dystrophin-deficient myotubes (Fig. 8e). A random and punctuate distribution was observed for all calcium transporters (not shown) in SolD7 myotubes without any obvious differences with dystrophin-deficient cells. This suggests that the different spatial distribution of spontaneous calcium events cannot be attributed to differences in distribution of calcium channels and calcium pumps from the SR (DHPR and RYR and SERCA) or to major differences in amounts and localization of coupling sites (colocalization of DHPR and RYR). These similar patterns in the distribution of calcium transporters is also indicating that age-matched sol8 myotubes are reaching similar developing stages independently of the forced expression of minidystrophin. Myotubes never reached stages where calcium transporters are aligned on transversal striation. Similarly, morphologic analysis and staining of myofilaments by labelling troponin-T (Figs. 8g, h) showed that both population reached the same differentiated stage characterized by long myotubes (sometimes branched) with centrally located nuclei and nascent myofilaments arranged as long parallel bundles aligned in the longitudinal axis of myotubes (Figs. 8g, h). Sol8 myotubes did not further differentiate into striated myotubes independently of the expression of minidystrophin. Both populations of myotubes remained poorly contractile when stimulated by the patch clamp technique (only 30% of myotubes responding against 80% in primary culture), and spontaneous contractile activity was usually absent. Total cell lysates were also applied at the same amount of protein and migrated in parallel for comparing by Western blotting the expression levels of the β-enolase (Fig. 8i) and of troponin-T (Fig. 8j), two markers of myogenic differentiation. For troponin-T levels, results were expressed as ratio of densities from bands of troponin-T over densities from bands of α-tubulin, taken as an internal control. The densitometric analysis of bands revealed that the differentiation markers were all expressed at the same level in all myotubes populations (Figs. 8i, j). This showed that aged-matched myotubes expressing minidystrophin or deficient in dystrophin displayed similar differentiated stages.

Discussion

Several studies have examined the functional consequences of dystrophin expression at the sarcolemma of muscle fibres from transgenic *mdx* mice expressing mini- [8,10] or full-length dystrophin [46–48]. These studies report gains on mechanical properties and sarcolemmal stability, recovery of the DAPs at the sarcolemma, and elimination of dystrophic symptoms. Indeed, little information exists concerning changes on calcium regulation after restoration of dystrophin expression. Recovery of low-resting $[Ca^{2+}]_i$ in transgenic *mdx* mice expressing full-length dystrophin [25] and after liposome-mediated transfection of the full-length dystrophin cDNA in *mdx*-cultured myotubes has been previously reported [32]. Our data obtained from Sol8 microinjected myotubes confirm this first observation. Transient expression of full-length dystrophin in microinjected Sol8 myotubes originally exhibiting severe alteration of calcium homeostasis significantly decreased resting $[Ca^{2+}]_i$. The lowering of steady-state levels of cytosolic calcium ions appeared rapidly only 2 days after transfection, and was more pronounced after 4 days at differentiation stage F+6. The previous works on *mdx* muscle cells [25,32] demonstrated that lowering of the resting $[Ca^{2+}]_i$ was accompanied with decreased activity of sarcolemmal leak calcium channels. Here, we show that recovery of calcium handling by full-length dystrophin is also involving the reduction of the amplitude of transient increase in cytoplasmic activity during depolarization (Figs. 5c, d). These calcium transients are due to the calcium release from the sarcoplasmic reticulum, since it is blocked by ryanodine (not shown). Moreover, preliminary results showed a reduction of the amplitude of calcium transients when calcium release from ryanodine receptors opening was more directly triggered by caffeine ($\Delta[Ca^{2+}]_i$ was 550 nM in SolC1 myotubes against 175 nM in SolD7 myotubes). This suggested that recovery of calcium handling is accompanied by a tighter regulation of calcium release from ryanodine and caffeine-activated stores.

Additionally to transient expression of full-length dystrophin, we analyzed a second experimental model based on the selection of stable Sol8 subclones (SolD7 and SolD6) constitutively expressing the BMD minidystrophin lacking a large portion of the central rod domain. The results obtained show that minidystrophin leads to apparent normal sarcolemmal expression and location of several members of the DAPs complex. Indeed, the present study indicates that minidystrophin forced expression can support accumulation of members of DAPs complex, that is, γ-sarcoglycan and α-dystrobrevin-1, at the sarcolemma. Among the DAPs tested, we have observed that α-sarcoglycan is not expressed in Sol8 myotubes and even in SolD7 line after minidystrophin

sarcolemmal restoration. This could be explained by a delayed expression of sarcoglycans compared to dystroglycans, as observed in cultured myotubes of a subclone of the mouse C2C12 myogenic cell line, where α-sarcoglycan aroused from F+4 [38]. It can be hypothesized that Sol8 cell line and its subclones die before reaching a sufficient differentiated stage to express α-sarcoglycan. The expression of γ-sarcoglycan at the sarcolemma in absence of α-sarcoglycan is surprising, since it is generally admitted that all four sarcoglycans must be co-expressed for proper cell surface localization [49]. The existence of a ε-sarcoglycan-containing sarcoglycan complex [50] may explain why residual levels of sarcoglycan expression are seen in myotubes with α-sarcoglycan deficiency.

The lowering of resting $[Ca^{2+}]_i$ observed after transient transfection of full-length dystrophin was also observed in F+4 and F+5 myotubes constitutively expressing BMD minidystrophin. This difference could be observed only at stages where differentiated myotubes still looked healthy, and the resting $[Ca^{2+}]_I$ of SolD7 myotubes, (and also of the two other clones SolD5 and SolD6) at F+4 and F+5, stages was closer to the levels observed in primary cultures. This effect was however not observed at later stages, which could suggest at first sight that the effect of minidystrophin is transitory. However, other observations suggest that Sol8 myotubes may develop additional severe alteration of calcium homeostasis at the end of their in vitro life independently of the presence of minidystrophin. A major dying process which occurred at late stages in SolC1 cell lines (between F+5 and F+6 days) may interfere with calcium measurement and lead to an underestimation of mean values, since numerous dying myotubes have detached at this stage. On the contrary, major occurrence of necrotic myotubes was delayed in minidystrophin-expressing cells (between F+6 and F+7 days). This may explain why additional calcium handling disregulation preceding calcium cell death could be observed at day 6 before major detachment at day 7.

Nevertheless, the results showed that BMD minidystrophin forced expression was able to regulate more tightly intracellular calcium handling during the first stages of differentiation comparing to dystrophin-deficient cells. Since the levels of resting calcium activity are also dependent on the differentiation stage, we had to take care in comparing age-matched myotubes similar in morphology and from cultures performed in parallel. The analysis of calcium transporters and myofilaments distribution, as well as the levels of differentiation markers like troponin-T suggested that both populations of myotubes were at the same differentiation stage independently of minidystrophin expression. Both populations of myotubes never reach striated differentiated stages with significant contractile activity. In addition to an absence of effect of minidystrophin on differentiation, these observations emphasize that differences in calcium homeostasis were obtained in absence of contractile activity and mechanical stimulations.

The relatively small difference in resting calcium after minidystrophin overexpression (between 20 and 30 nM) was very reminiscent of values obtained in previous studies. When measured in cultured myotubes from normal muscles or dystrophic muscles, a very similar difference of 22 nM in resting calcium activity was observed at 10 days of coculture between normal and DMD cocultured human myotubes [30]. Other authors [51] reported similar differences after 4 to 8 days of differentiation in human myotubes (29 nM between normal and DMD) and mouse myotubes (29 nM between normal and *mdx*). After lipofection of a cDNA plasmid encoding for full-length dystrophin, the difference in resting calcium activity was 10 nM between transfected and non-transfected *mdx* myotubes [32]. These moderate differences in resting calcium activity reveal sustained and global differences in free calcium ions levels that can have significant chronic effects in dystrophic cells. This difference in average calcium levels also suggests that, in various subcellular compartments (for instance underneath the membrane), calcium ions can be much more elevated and can have more acute effects.

The analysis of intracellular calcium signalling showed that calcium release was more tightly regulated in minidystrophin-expressing cells. The depolarization-induced transients, through 100-mM KCl stimulation, resulted in a lower response amplitude in both mini- and full-length dystrophin-positive myotubes, in comparison to their controls. The same observation has been done in control and DMD human cultured [52] and co-cultured [30] myotubes, where amplitude of calcium transients was found to be higher in dystrophin-deficient DMD myotubes, compared to the dystrophin-positive control ones. Other results showed that calcium transients were similar in control and *mdx* fibres in response to electrically induced membrane depolarization [19,53]. However, the use of targeted aequorin revealed higher calcium transients in mitochondria of *mdx* myotubes and in the cytosol at later stages of culture [31]. Our results and those obtained in human muscle cells strongly suggest that dystrophin could directly or indirectly interact with and/or regulate one or several calcium transport mechanisms in muscle cells, but the mechanisms by which Ca^{2+} transients are altered remains elusive. Measurements obtained with SR targeted aequorin suggested an overload of intraluminal $[Ca^{2+}]$ in *mdx* myotubes [31]. It is possible that equilibrium between a higher steady-state level of free cytosolic calcium results in a higher loading of SR stores and, in turn, in increased calcium-release peaks during depolarization of dystrophin-deficient cells. In another hand, expression of dystrophin may influence the functioning of calcium-release channels by changing their cellular environment in terms of distribution, association with other cytoskeleton or regulatory proteins or by changing the balance of expression of calcium channels isoforms. Since dystrophin could also regulate the activity of various sarcolemmal channels transporting calcium entries, changes in these influxes could be indirectly involved in changes of

calcium-release activity by modulation of the calcium-induced calcium-release properties and of excitability of SR channels.

BMD minidystrophin expression had not only consequences on the properties of calcium signalling during a depolarization but also on the pattern of spontaneous calcium-release events. Normal skeletal muscle cells have to maintain a low free calcium concentration at rest to remain excitable and viable. In accordance with this idea, minidystrophin-expressing myotubes are exhibiting few, discrete, and space-restricted spontaneous calcium release at rest. On the contrary, the spontaneous calcium-release activity often led to intense and propagating calcium events in dystrophin-deficient myotubes sometimes evolving as calcium waves. Our preliminary results show that minidystrophin-expressing myotubes display a pattern of calcium-release events similar to the one observed in primary cultures. This suggests that BMD minidystrophin is thus able to restore a normal calcium-release behaviour. However, it is not possible to determine if the prevention of spontaneous propagating activities is due to secondary effects of the lower steady-state level of calcium ions in cytosol, or to changes in expression pattern of channels or in direct functional regulation by sarcolemmal calcium influx or cytoskeleton proteins. For instance, Zhou et al. [54] reported a 4.8-fold increase in event frequency when $[Ca^{2+}]_i$ was greatly elevated from 100 to 400 nM. According to CSLM studies and to immunostaining of calcium channels and transporters, the differences in calcium-release pattern are not due to obvious changes in the subcellular distribution of these calcium-signalling proteins. Functional parameters and protein expression pattern have thus to be explored and the sparks activities have to be more deeply studied. Changes in spontaneous calcium-release events after mini dystrophin expression could also be explained by changes in mitochondria activity. Indeed, a recent study suggested that mitochondria exert a negative control over calcium-release event frequency [55].

The present approach provides the opportunity to explore changes in calcium transport mechanisms through the sarcolemma or organelle membranes after dystrophin forced expression. A previous study from McCarter et al. [32] has shown that the mean open probability of calcium leak channels was reduced to a level similar to normal mouse myotubes, when *mdx* muscle cells were transfected with a plasmid containing the full-length dystrophin cDNA. Other candidates for transporting significant calcium amounts like store-operated calcium entries could be interrogated with sensitive techniques. Alterations of the calcium influx in dystrophin-deficient myotubes may be only one of the aspects leading to the alteration of the global resting $[Ca^{2+}]_i$. Obviously, compensation of this increased influx by the intracellular buffering system are likely altered in dystrophin-deficient cells since persistent increase of the steady-state level of calcium ions can be observed in cytosol. Other cellular compartments involved in calcium handling should also be explored, such as restricted domains of elevated $[Ca^{2+}]$ at the subsarcolemmal level [56] or within mitochondria [31]. Sol8 cells and their subclones could be relevant supports to study Ca^{2+} accumulation in these microdomains in both absence and presence of dystrophin or truncated dystrophins comparatively. Although the behaviour of releasable SR calcium stores seems to be affected, the study of the calcium handling abilities of the mitochondrion is also very pertinent, since it may lead to alteration of the ATP metabolism and calcium influx as well as spontaneous calcium-release activity.

The approach of dystrophin cDNA transfer has permit to demonstrate an effect of BMD minidystrophin and full-length dystrophin expression on calcium handling and calcium-signalling properties of cultured skeletal muscle cells. Significant changes in calcium signalling appeared as a better control of releasable pool of calcium ions from the SR.

Restoration of calcium handling with dystrophin occurred rapidly in 2–3 days of culture, which suggests that this is not a secondary consequence dependent on the history of myotubes. It has to be noted that utrophin is expressed in the dystrophin-deficient myotubes at similar levels than in minidystrophin-transfected cells. This indicates that this dystrophin-related protein do not compensate for the absence of dystrophin in calcium handling. A direct link may exist between dystrophin-based cytoskeleton and intracellular systems involved in calcium regulation. The effects of BMD minidystrophin, notably on calcium-release events, also suggest that the central rod domain of 427 kDa dystrophin is not crucial for the interactions with the intracellular calcium-signalling apparatus. These cellular models will help to determine which systems are directly dependent on dystrophin expression among the SR, mitochondria, and sarcolemmal channels. Our previous study conducted in cocultured human myotubes led to the idea of alteration dependent on the contraction [30] and changes in activity of stretch-activated channels [22]. The present data obtained in Sol8 myotubes that do not reach contractile differentiated stage suggests that dystrophin and minidystrophin are able to regulate calcium transporters that are present at early stages of differentiation and independent on the appearance of contractility.

Acknowledgments

The authors thank Pr. Isabelle Martelly (University of Paris XII, Créteil, France) for providing original Sol8 cell line. We thank Dr. Stanley C. Froehner (University of North Carolina, USA) for polyclonal antibodies against α_1-syntrophin, α-dystrobrevin 1 and α-dystrobrevin 2. This work was financially supported by grants from Centre National de la Recherche Scientifique (CNRS UMR 6558), University of Poitiers and the Association Française contre les Myopathies. Dr. Eric Marchand had a fellowship from

the Région Poitou-Charentes. We thank Françoise Mazin for expert technical assistance in cell culture.

References

[1] K. Arahata, S. Ishiura, T. Ishiguro, T. Tsukahara, Y. Suhara, C. Eguchi, T. Ishihara, I. Nonaka, E. Ozawa, H. Sugita, Immunostaining of skeletal and cardiac muscle surface membrane with antibody against Duchenne muscular dystrophy peptide, Nature 333 (1988) 861–863.
[2] V. Straub, K.P. Campbell, Muscular dystrophies and the dystrophin–glycoprotein complex, Curr. Opin. Neurol. 10 (1997) 168–175.
[3] M. Yoshida, E. Ozawa, Glycoprotein complex anchoring dystrophin to sarcolemma, J. Biochem. (Tokyo) 108 (1990) 748–752.
[4] J.M. Ervasti, K.P. Campbell, Membrane organization of the dystrophin–glycoprotein complex, Cell 66 (1991) 1121–1131.
[5] J.M. Ervasti, K.P. Campbell, A role for the dystrophin–glycoprotein complex as a transmembrane linker between laminin and actin, J. Cell Biol. 122 (1993) 809–823.
[6] M. Koenig, E.P. Hoffman, C.J. Bertelson, A.P. Monaco, C. Feener, L.M. Kunkel, Complete cloning of the Duchenne muscular dystrophy (DMD) cDNA and preliminary genomic organization of the DMD gene in normal and affected individuals, Cell 50 (1987) 509–517.
[7] S.B. England, L.V. Nicholson, M.A. Johnson, S.M. Forrest, D.R. Love, E.E. Zubrzycka-Gaarn, D.E. Bulman, J.B. Harris, K.E. Davies, Very mild muscular dystrophy associated with the deletion of 46% of dystrophin, Nature 343 (1990) 180–182.
[8] N. Deconinck, T. Ragot, G. Marechal, M. Perricaudet, J.M. Gillis, Functional protection of dystrophic mouse (mdx) muscles after adenovirus-mediated transfer of a dystrophin minigene, Proc. Natl. Acad. Sci. U. S. A. 93 (1996) 3570–3574.
[9] A. Decrouy, J.M. Renaud, H.L. Davis, J.A. Lunde, G. Dickson, B.J. Jasmin, Mini-dystrophin gene transfer in mdx4cv diaphragm muscle fibers increases sarcolemmal stability, Gene Ther. 4 (1997) 401–408.
[10] K. Yuasa, Y. Miyagoe, K. Yamamoto, Y. Nabeshima, G. Dickson, S. Takeda, Effective restoration of dystrophin-associated proteins in vivo by adenovirus-mediated transfer of truncated dystrophin cDNAs, FEBS Lett. 425 (1998) 329–336.
[11] P.R. Turner, T. Westwood, C.M. Regen, R.A. Steinhardt, Increased protein degradation results from elevated free calcium levels found in muscle from mdx mice, Nature 335 (1988) 735–738.
[12] J.B. Bodensteiner, A.G. Engel, Intracellular calcium accumulation in Duchenne dystrophy and other myopathies: a study of 567,000 muscle fibers in 114 biopsies, Neurology 28 (1978) 439–446.
[13] C.J. Duncan, Role of intracellular calcium in promoting muscle damage: a strategy for controlling the dystrophic condition, Experientia 34 (1978) 1531–1535.
[14] T.E. Bertorini, S.K. Bhattacharya, G.M. Palmieri, C.M. Chesney, D. Pifer, B. Baker, Muscle calcium and magnesium content in Duchenne muscular dystrophy, Neurology 32 (1982) 1088–1092.
[15] M.J. Jackson, D.A. Jones, R.H. Edwards, Measurements of calcium and other elements in muscle biopsy samples from patients with Duchenne muscular dystrophy, Clin. Chim. Acta 147 (1985) 215–221.
[16] P.R. Turner, P.Y. Fong, W.F. Denetclaw, R.A. Steinhardt, Increased calcium influx in dystrophic muscle, J. Cell Biol. 115 (1991) 1701–1712.
[17] N. Imbert, C. Vandebrouck, B. Constantin, G. Duport, C. Guillou, C. Cognard, G. Raymond, Hypoosmotic shocks induce elevation of resting calcium level in Duchenne muscular dystrophy myotubes contracting in vitro, Neuromuscular Disord. 6 (1996) 351–360.
[18] F.W. Hopf, P.R. Turner, W.F. Denetclaw Jr., P. Reddy, R.A. Steinhardt, A critical evaluation of resting intracellular free calcium regulation in dystrophic mdx muscle, Am. J. Physiol. 271 (1996) C1325–C1339.
[19] O. Tutdibi, H. Brinkmeier, R. Rudel, K.J. Fohr, Increased calcium entry into dystrophin-deficient muscle fibres of MDX and ADR-MDX mice is reduced by ion channel blockers, J. Physiol. 515 (1999) 859–868.
[20] A. Franco Jr., J.B. Lansman, Calcium entry through stretch-inactivated ion channels in mdx myotubes, Nature 344 (1990) 670–673.
[21] P.Y. Fong, P.R. Turner, W.F. Denetclaw, R.A. Steinhardt, Increased activity of calcium leak channels in myotubes of Duchenne human and mdx mouse origin, Science 250 (1990) 673–676.
[22] C. Vandebrouck, G. Duport, C. Cognard, G. Raymond, Cationic channels in normal and dystrophic human myotubes, Neuromuscular Disord. 11 (2001) 72–79.
[23] C. Vandebrouck, D. Martin, M. Colson-Van Schoor, H. Debaix, P. Gailly, Involvement of TRPC in the abnormal calcium influx observed in dystrophic (mdx) mouse skeletal muscle fibers, J. Cell Biol. 158 (2002) 1089–1096.
[24] A.J. Bakker, S.I. Head, D.A. Williams, D.G. Stephenson, Ca2+ levels in myotubes grown from the skeletal muscle of dystrophic (mdx) and normal mice, J. Physiol. 460 (1993) 1–13.
[25] W.F. Denetclaw Jr., F.W. Hopf, G.A. Cox, J.S. Chamberlain, R.A. Steinhardt, Myotubes from transgenic mdx mice expressing full-length dystrophin show normal calcium regulation, Mol. Biol. Cell 5 (1994) 1159–1167.
[26] P. Gailly, B. Boland, B. Himpens, R. Casteels, J.M. Gillis, Critical evaluation of cytosolic calcium determination in resting muscle fibres from normal and dystrophic (mdx) mice, Cell Calcium 14 (1993) 473–483.
[27] S.I. Head, Membrane potential, resting calcium and calcium transients in isolated muscle fibres from normal and dystrophic mice, J. Physiol. 469 (1993) 11–19.
[28] J. Pressmar, H. Brinkmeier, M.J. Seewald, T. Naumann, R. Rudel, Intracellular Ca2+ concentrations are not elevated in resting cultured muscle from Duchenne (DMD) patients and in MDX mouse muscle fibres, Pfluegers Arch. 426 (1994) 499–505.
[29] M. Rivet-Bastide, N. Imbert, C. Cognard, G. Duport, Y. Rideau, G. Raymond, Changes in cytosolic resting ionized calcium level and in calcium transients during in vitro development of normal and Duchenne muscular dystrophy cultured skeletal muscle measured by laser cytofluorimetry using indo-1, Cell Calcium 14 (1993) 563–571.
[30] N. Imbert, C. Cognard, G. Duport, C. Guillou, G. Raymond, Abnormal calcium homeostasis in Duchenne muscular dystrophy myotubes contracting in vitro, Cell Calcium 18 (1995) 177–186.
[31] V. Robert, M.L. Massimino, V. Tosello, R. Marsault, M. Cantini, V. Sorrentino, T. Pozzan, Alteration in calcium handling at the subcellular level in mdx myotubes, J. Biol. Chem. 276 (2001) 4647–4651.
[32] G.C. McCarter, W.F. Denetclaw Jr., P. Reddy, R.A. Steinhardt, Lipofection of a cDNA plasmid containing the dystrophin gene lowers intracellular free calcium and calcium leak channel activity in mdx myotubes, Gene Ther. 4 (1997) 483–487.
[33] W.X. Guo, M. Nichol, J.P. Merlie, Cloning and expression of full length mouse utrophin: the differential association of utrophin and dystrophin with AChR clusters, FEBS Lett. 398 (1996) 259–264.
[34] E. Marchand, B. Constantin, C. Vandebrouck, G. Raymond, C. Cognard, Calcium homeostasis and cell death in Sol8 dystrophin-deficient cell line in culture, Cell Calcium 29 (2001) 85–96.
[35] N. Imbert, C. Vandebrouck, G. Duport, G. Raymond, A.A. Hassoni, B. Constantin, M.J. Cullen, C. Cognard, Calcium currents and transients in co-cultured contracting normal and Duchenne muscular dystrophy human myotubes, J. Physiol. 534 (2001) 343–355.
[36] C. Mulle, P. Benoit, C. Pinset, M. Roa, J.P. Changeux, Calcitonin gene-related peptide enhances the rate of desensitization of the nicotinic acetylcholine receptor in cultured mouse muscle cells, Proc. Natl. Acad. Sci. U. S. A. 85 (1988) 5728–5732.
[37] Y.M. Chan, C.G. Bonnemann, H.G. Lidov, L.M. Kunkel, Molecular organization of sarcoglycan complex in mouse myotubes in culture, J. Cell Biol. 143 (1998) 2033–2044.
[38] S. Noguchi, E. Wakabayashi, M. Imamura, M. Yoshida, E. Ozawa, Developmental expression of sarcoglycan gene products in cultured myocytes, Biochem. Biophys. Res. Commun. 262 (1999) 88–93.
[39] M.F. Peters, M.E. Adams, S.C. Froehner, Differential association of

syntrophin pairs with the dystrophin complex, J. Cell Biol. 138 (1997) 81–93.
[40] M.E. Adams, N. Kramarcy, S.P. Krall, S.G. Rossi, R.L. Rotundo, R. Sealock, S.C. Froehner, Absence of alpha-syntrophin leads to structurally aberrant neuromuscular synapses deficient in utrophin, J. Cell Biol. 150 (2000) 1385–1398.
[41] G. Grynkiewicz, M. Poenie, R.Y. Tsien, A new generation of Ca2+ indicators with greatly improved fluorescence properties, J. Biol. Chem. 260 (1985) 3440–3450.
[42] C. Cognard, B. Constantin, M. Rivet-Bastide, G. Raymond, Intracellular calcium transients induced by different kinds of stimulus during myogenesis of rat skeletal muscle cells studied by laser cytofluorimetry with Indo-1, Cell Calcium 14 (1993) 333–348.
[43] F.A. Lattanzio Jr., The effects of pH and temperature on fluorescent calcium indicators as determined with Chelex-100 and EDTA buffer systems, Biochem. Biophys. Res. Commun. 171 (1990) 102–108.
[44] L.A. Blatter, W.G. Wier, Intracellular diffusion, binding, and compartmentalization of the fluorescent calcium indicators indo-1 and fura-2, Biophys. J. 58 (1990) 1491–1499.
[45] L. Hove-Madsen, D.M. Bers, Indo-1 binding to protein in permeabilized ventricular myocytes alters its spectral and Ca binding properties, Biophys. J. 63 (1992) 89–97.
[46] K. Matsumura, C.C. Lee, C.T. Caskey, K.P. Campbell, Restoration of dystrophin-associated proteins in skeletal muscle of mdx mice transgenic for dystrophin gene, FEBS Lett. 320 (1993) 276–280.
[47] G.A. Cox, N.M. Cole, K. Matsumura, S.F. Phelps, S.D. Hauschka, K.P. Campbell, J.A. Faulkner, J.S. Chamberlain, Overexpression of dystrophin in transgenic mdx mice eliminates dystrophic symptoms without toxicity, Nature 364 (1993) 725–729.
[48] D.J. Wells, K.E. Wells, E.A. Asante, G. Turner, Y. Sunada, K.P. Campbell, F.S. Walsh, G. Dickson, Expression of human full-length and minidystrophin in transgenic mdx mice: implications for gene therapy of Duchenne muscular dystrophy, Hum. Mol. Genet. 4 (1995) 1245–1250.
[49] K.H. Holt, K.P. Campbell, Assembly of the sarcoglycan complex. Insights for muscular dystrophy, J. Biol. Chem. 273 (1998) 34667–34670.
[50] L.A. Liu, E. Engvall, Sarcoglycan isoforms in skeletal muscle, J. Biol. Chem. 274 (1999) 38171–38176.
[51] W.F. Denetclaw, G. Bi, D.V. Pham, R.A. Steinhardt, Heterokaryon myotubes with normal mouse and Duchenne nuclei exhibit sarcolemmal dystrophin staining and efficient intracellular free calcium control, Mol. Biol. Cell 4 (1993) 963–972.
[52] T. Mongini, D. Ghigo, C. Doriguzzi, F. Bussolino, G. Pescarmona, B. Pollo, D. Schiffer, A. Bosia, Free cytoplasmic Ca++ at rest and after cholinergic stimulus is increased in cultured muscle cells from Duchenne muscular dystrophy patients, Neurology 38 (1988) 476–480.
[53] C. Collet, B. Allard, Y. Tourneur, V. Jacquemond, Intracellular calcium signals measured with indo-1 in isolated skeletal muscle fibres from control and mdx mice, J. Physiol. 520 (Pt 2) (1999) 417–429.
[54] J. Zhou, A. Gonzalez, R. Segura, E. Rios, G. Ferreira, J. Yi, G. Brum, Modulation by Ca^{2+} and Mg^{2+} of mammalian muscle Ca^{2+} sparks, Biophys. J. 82 (2002) 510A.
[55] E.V. Isaeva, N. Shirokova, Metabolic regulation of Ca2+ release in permeabilized mammalian skeletal muscle fibres, J. Physiol. 547 (2003) 453–462.
[56] N. Mallouk, V. Jacquemond, B. Allard, Elevated subsarcolemmal Ca2+ in mdx mouse skeletal muscle fibers detected with Ca2+-activated K+ channels, Proc. Natl. Acad. Sci. U. S. A. 97 (2000) 4950–4955.